Conformation-Specific Pathways of β-Alanine: A Vacuum Ultraviolet Photoionization and Theoretical Study

Lidong Zhang, Yang Pan, Huijun Guo, Taichang Zhang, Liusi Sheng, and Fei Qi*

National Synchrotron Radiation Laboratory, University of Science and Technology of China, Hefei, Anhui230029, P. R. China

Po-Kam Lo and Kai-Chung Lau*

Department of Biology and Chemistry, City University of Hong Kong, Tat Chee Avenue, Kowloon, Hong Kong, P. R. China

Received: January 11, 2009; Revised Manuscript Received: April 7, 2009

We report a photoionization and dissociative photoionization study of β-alanine using IR laser desorption combined with synchrotron vacuum ultraviolet (VUV) photoionization mass spectrometry. Fragments at m/z = 45, 44, 43, and 30 yielded from photoionization are assigned to $NH_3CH_2CH_2^+$, $NH_2CHCH_3^+$, $NH_2CHCH_2^+$, and $NH_2CH_2^+$, respectively. Some new conformation-specific dissociation channels and corresponding dissociation energies for the observed fragments are established and determined with the help of *ab initio* G3B3 calculations and measurements of photoionization efficiency (PIE) spectra. The theoretical values are in fair agreement with the experimental results. Three low-lying conformers of the β-alanine cation, including two *gauche* conformers G1+, G2+ and one *anti* conformer A+ are investigated by G3B3 calculations. The conformer G1+ (intramolecular hydrogen bonding N−H···O═C) is found to be another precursor in forming the $NH_3CH_2CH_2^+$ ion, which is complementary to the previously reported formation pathway that only occurs with the conformer G2+ (intramolecular hydrogen bonding O−H···N). Species $NH_2CHCH_2^+$ may come from the contributions of G1+, G2+, and A+ via different dissociation pathways. The most abundant fragment ion, $NH_2CH_2^+$, is formed from a direct C−C bond cleavage. Intramolecular hydrogen transfer processes dominate most of the fragmentation pathways of the β-alanine cation.

1. Introduction

Various conformers can coexist under ambient conditions for most amino acids. Interconversions among these conformers occur easily even at low temperatures due to the low energetic barriers. Conformation-specific reaction mechanisms have been established before,[1] but direct verification of them is difficult because of the quick interconversion processes, especially with thermal activation.[2] Recent studies demonstrate that the different photodissociation channels and chemical reactivity of various conformers for a given molecule can be understood by selective laser control of chemical reactions.[2−6] Park et al. have reported the selective generation of *gauche*-1-iodopropane and *anti*-1-iodopropane using mass-analyzed threshold ionization (MATI) and direct observation of conformation-specific pathways in the photodissociation of 1-iodopropane ions.[4] Another experiment has shown that the photodissociation of *trans* and *cis* forms of formic acid in solid Ar yields products H_2O + CO and H_2 + CO_2, respectively.[5] These results demonstrate that a chemical reaction may be controlled by selectively preparing a particular conformer of the reactants. In addition, direct measurement of energy thresholds to conformational isomerization in tryptamine has also been achieved via a vibrational excitation scheme named stimulated emission thresholds (SEP).[7]

Amino acids, among the most important building blocks of life, are believed to play key roles in space chemistry and the origin of life on the earth.[8,9] Photoionization and dissociative photoionization investigations of amino acids, especially in the vacuum ultraviolet (VUV) range in the gas phase, also appear to be worthwhile.[10−13] As the simplest β-amino acid, β-alanine is found to be the most abundant amino acids existing in CI chondrites, a type of carbonaceous meteorite.[14] Because of the flexibility in the molecular backbone of β-alanine, a large number of low-lying torsional conformers have been investigated in the gas phase by experimental and computational methods.[15−17] Recently, two new conformers were identified using Fourier transform microwave spectroscopy,[16] in addition to the known *gauche* conformers, named G1 and G2.[17] For the two new conformers, a *gauche* conformer G3 with an intramolecular hydrogen bond between the amino group and carbonyl oxygen (N−H···O═C) is established, while another *anti* conformer A stabilized by an $n-\pi^*$ hyperconjugative interaction between the nucleophile N: of the amino group and the π^* orbital at the carbonyl group has also been presented. Ionization of β-alanine gives rise to a series of fragments. It is noted that comprehensive investigations of β-alanine, especially on conformation-specific ionization and dissociation processes in the gas phase, are still rare. To the best of our knowledge, there have been only three photoionization studies of β-alanine.[18−20] Jochims et al. studied the photoionization characters of β-alanine in the 6−22 eV photon energy range, but the assignments of the fragments at m/z = 44 ($NH_2CH_2CH_2^+$) and 45 ($COOH^+$) at low photon energy (<11.8 eV) are controversial.[18,20] Choi et al. thought that the fragment ion at m/z = 45 ($NH_3CH_2CH_2^+$) is formed via a highly conformation-specific decarboxylation pathway of β-alanine. Unfortunately, they did not observe the signal of m/z =

* Corresponding author. E-mail: fqi@ustc.edu.cn (F.Q.); kaichung@cityu.edu.hk (K.-C.L.).

10.1021/jp9002565 CCC: $40.75
Published on Web 04/28/2009

30 ($NH_2CH_2^+$) in the mass spectrum obtained at the photon energy of 9.35 eV, a predominant fragment ion that can be produced easily under such photon energy.[19] Moreover, the reported appearance energy of $NH_3CH_2CH_2^+$ is too low, which is just a little higher than the ionization energy (8.93 eV) of β-alanine. More recently, Bari et al. reported the fragmentation of α- and β-alanine induced by multiply charged ions at Bragg-peak energies. A series of fragments are formed in double ionization.[21]

Recently, we have used IR laser desorption/tunable synchrotron VUV photoionization mass spectrometry (IR LD/VUV PIMS) technique to investigate the fragmentation pathways of α-alanine.[22] The dissociation reactions of the α-alanine and β-alanine cation radicals have a large difference.[18,19] In this work, we present the photoionization and dissociative photoionization studies of β-alanine, an isomer of α-alanine. Photoionization mass spectra of β-alanine at different photon energies are obtained. Ionization energy (IE) of the parent and appearance energies (AEs) of some fragments are determined by measurements of photoionization efficiency (PIE) spectra. Complementary *ab initio* calculations at the G3B3 level have been performed. The theoretical results are used to discuss and explain the conformation-specific photodissociation pathways for the fragments $NH_3CH_2CH_2^+$, $NH_2CHCH_3^+$, $NH_2CHCH_2^+$, and $NH_2CH_2^+$, with *m*/*z* ratios 45, 44, 43, and 30, respectively.

2. Experimental and Theoretical Methods

2.1. Experimental Method. The IR LD/VUV PIMS instrument has been reported elsewhere.[22−25] Hence, only a short description is given here. Synchrotron radiation from an undulator beamline of the 800 MeV electron storage ring of National Synchrotron Radiation Laboratory at Hefei, China is monochromatized with a 1 m Seya-Namioka monochromator equipped with a laminar grating (1500 grooves/mm, Horiba Jobin Yvon, France). This grating covers the photon energy from 7.8 to 24 eV. The monochromator is calibrated with the known ionization energies of the inert gases. The energy resolving power ($E/\Delta E$) is about 1000. A gas filter filled with argon is used to eliminate higher order harmonic radiation in this study. The average photon flux can reach the magnitude of 10^{13} photons/s. A silicon photodiode (SXUV-100, International Radiation Detectors, Inc., USA) is used to monitor the photon flux for normalizing ion signals.

The experiments utilize 1064 nm output of a pulsed Nd:YAG laser (Surelite I-20, Continuum, USA) for IR laser desorption. Laser power at the surface of substrate is controlled at 10 mJ/pulse to generate intact neutral molecules for near-threshold VUV photoionization. The VUV light beam is perpendicular and overlapping to the IR laser beam in the photoionization region. VUV photoionization takes place at a distance of 2−4 mm from the substrate surface, where the plume of molecules formed from the desorption process travels back and is ionized by VUV light. Ions produced by VUV light are analyzed by a reflectron time-of-flight (TOF) mass spectrometer. A pulsed voltage of 260 V applied to the repeller plates is used to propel ions into the flight tube. The pulsed voltage with the frequency of 10 kHz works with a delay of 150 μs after the laser fires with the frequency of 10 Hz, which is controlled by a homemade pulse/delay generator.

The IR LD/VUV PIMS setup permits the laser irradiating onto the substrate coated with a layer of β-alanine, which was purchased from Fluka with the purity of ≥99.0% and used without further purification. To improve the signal intensity and decrease the background noise, stainless steel is selected as an ideal substrate without any organic matrix. The pressure of the photoionization chamber is around 1.0×10^{-4} Pa.

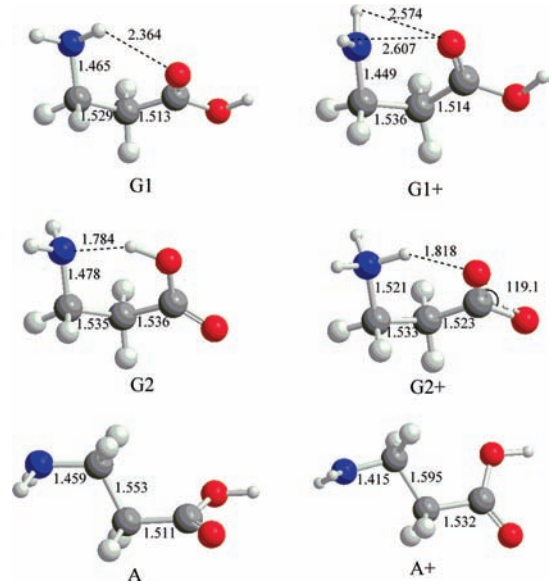

Figure 1. Optimized geometries of neutral molecules and ions of β-alanine at the B3LYP/6-31G(d) level (all distances in Å and all angles in degrees).

2.2. Computational Method. Some computational studies have been conducted on β-alanine previously; over 20 conformers in the gas phase have been reported.[17] At least three *gauche* conformers (G1, G2 and G3) and one *anti* conformer (A) are found to coexist in the gas phase.[15] In this work, the G3B3 calculations[26] were carried out with the Gaussian 03 program package.[27] It involves single-point calculations at the levels of QCISD(T,E4T)/6-31G(d), MP4/6-31+G(d), MP4/6-31G(2df,p), and MP2(Full)/G3large, based on the structures optimized at the B3LYP/6-31G(d) level. The B3LYP/6-31G(d) harmonic vibrational frequencies, scaled by 0.96, were used for the correction of zero-point vibrational energies (ZPVE). A semiempirical correction was also applied to account for the high level correlation effect. The correction is E (HLC, higher level correction) $= -An_\beta - B(n_\alpha - n_\beta)$ in the G3B3 theory, where n_α and n_β are the numbers of α and β valence electrons with $n_\alpha \geq n_\beta$. $A = 10.041$ mhartrees and $B = 4.995$ mhartrees for molecules; $A = 10.188$ mhartrees and $B = 2.323$ mhartrees for atoms.[26] A large number of molecules have been calculated using this method, and good correlation between the G3B3 method and experimental results has been found.[28,29] Optimized geometries of three typical low-lying conformers of β-alanine and corresponding cations are shown in Figure 1, including the *gauche* conformers G1 and G2 and the *anti* conformer A.[15] Conformer G3 has a configuration similar to that of G1, which is not shown here. The optimized geometries of the ions, transition states, and intermediates for the formation of $NH_2CH_2^+$, $NH_3CH_2CH_2^+$, $NH_2CHCH_3^+$, and $NH_2CHCH_2^+$ at the B3LYP/6-31G(d) level are displayed in Figures 2−3. The calculated energies E_0, and H_{298} (in hartrees) of various species involved in the dissociation of β-alanine at the G3B3 level are listed in Table 1. Adiabatic and vertical ionization energies were calculated to compare with our experimental results. The G3B3 vertical IEs are determined to be 9.75 and 11.1 eV for G1 and G2, respectively. The large energy discrepancy implies that the ejected electrons come from different function groups of G1 and G2. The highest occupied molecular orbital (HOMO) of G1 is the lone-pair orbital of the N atom (n_N), while the HOMO of G2 has strongly mixing $n_N + n_O$ characteristic.[15]

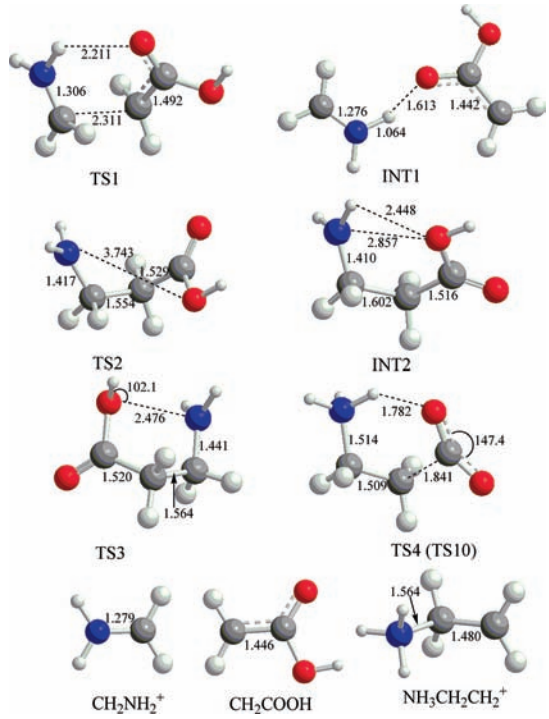

Figure 2. Optimized geometries of ions, transition states, and intermediates for the formation of $NH_2CH_2^+$ and $NH_3CH_2CH_2^+$ at the B3LYP/6-31G(d) level (all distances in Å and all angles in degrees).

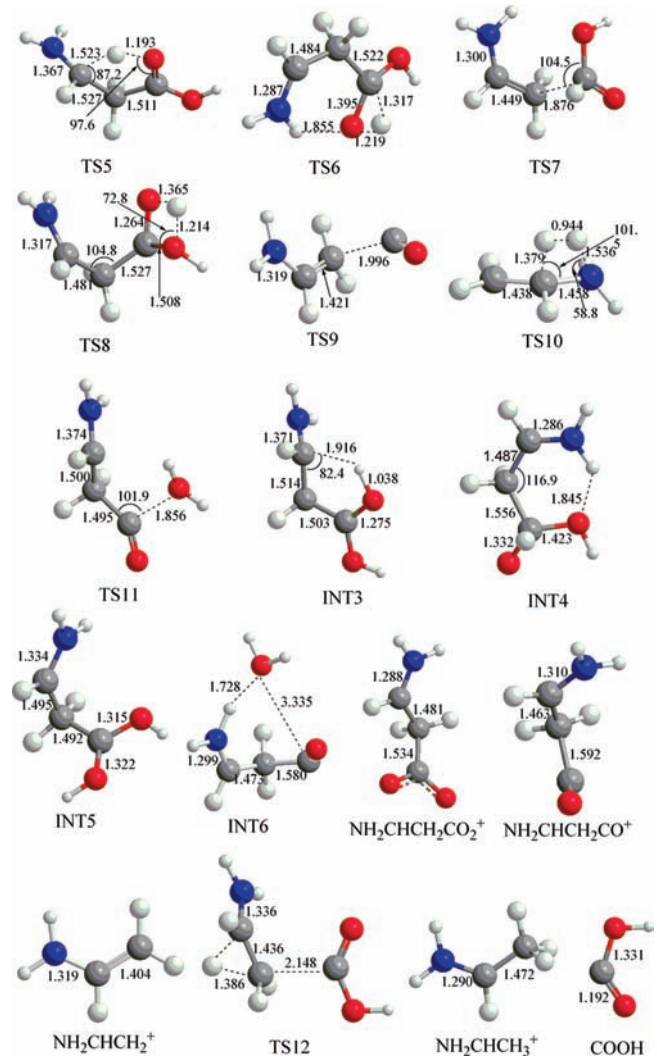

Figure 3. Optimized geometries of ions, transition states, and intermediates for the formation of $NH_2CHCH_2^+$ and $NH_2CHCH_3^+$ at the B3LYP/6-31G(d) level (all distances in Å and all angles in degrees).

3. Results and Discussion

3.1. Photoionization Mass spectra and Photoionization Efficiency Spectra. Figure 4a exhibits the photoionization mass spectra of β-alanine at the photon energies of 9.0 and 12.0 eV, respectively. A 10 mJ/pulse laser power was used in this study in order to avoid dissociation and ionization of β-alanine from the IR laser desorption process. Only exclusive parent ion at $m/z = 89$ is observed at the photon energy of 9.0 eV due to the near-threshold soft ionization. A variety of fragments are formed at higher photon energy, which was also found in previous studies.[18,30] Similar to the photoionization mass spectrum of glycine,[30] the most intense peak in the mass spectrum of β-alanine is observed at $m/z = 30$. Correspondingly, the intensity of the parent ion is very low, indicating that the dissociation of the parent cation requires only a small amount of internal energy.[18] Fragments at $m/z = 45$, 44, and 43 are also observed at higher photon energies of 9.5, 10.0, 11.0, and 12.0 eV with relative weak intensities, as shown in Figure 4b.

The IE value can be measured by scanning photoionization efficiency spectra, as that obtained from electron impact ionization (EI) studies. However, EI induced phenomena tend to be more complex, causing some difficulties in the interpretation of experimental data.[31] The PIE spectrum of β-alanine is obtained by plotting the integrated mass peak versus corresponding photon energy. The ion signals of parent ion ($m/z = 89$) increase monotonically with the photon energy, as shown in Figure 5a. In our experiments, desorbates from the laser desorption process are vibrationally hot and will cause a gradual onset at threshold. This so-called thermal tail may make it difficult to determine the onset accurately. Some methods have been employed for analyzing PIE spectra of polyatomic molecules.[32,33] Generally, the IE is determined by extrapolating the first linear rise in the PIE spectra. Although this baseline intercept method is somewhat rough, at least it is relatively straightforward. The IE of β-alanine is measured to be 8.86 ± 0.08 eV, which is similar to the previously reported experimental value (8.80 ± 0.1 eV)[18] and in good agreement with the G3B3 result (8.78 eV) for the ionization transition from β-alanine to *gauche* conformer G1+. On the potential energy surface of the β-alanine cation, we note that the lowest-energy cation has the form of $NH_3CHCH_2COOH^+$. Thus, the adiabatic IE of β-alanine should correspond to the ionization transition from β-alanine to $NH_3CHCH_2COOH^+$. At the G3B3 level, the adiabatic IE value of β-alanine is 8.51 eV. Nevertheless, the ionization threshold for β-alanine → $NH_3CHCH_2COOH^+$ may not be obvious in the PIE spectrum because of the poor Franck−Condon factor near the ionization threshold. The IE values for the ionization transitions from β-alanine to the G1+, G2+ and A+ conformers are listed in Table 2. The IE value from G2 to G2+ is 9.15 eV. The geometry has an obvious change from neutral to cation radical structure for G2. The G2 conformer has an OH---N hydrogen bond in the neutral form, but a NH---O hydrogen bond in the ionized form (Figure 1).[15] The AEs of major fragment ions at $m/z = 45$, 43, and 30, obtained by extrapolating the first linear rise from baseline in the PIE spectra (Figure 5b−d) together with the calculated G3B3 results, are also given in Table 2.

TABLE 1: G3B3 Energies E_0 and H_{298} (in hartrees) of Various Species Involved in the Dissociation of β-Alanine

species	E_0 (in hartrees)	H_{298} (in hartrees)
G1	−323.53041	−323.52268
G2	−323.52957	−323.52225
A	−323.52670	−323.51870
G1+	−323.20769	−323.20017
G2+	−323.19339	−323.18565
A+	−323.19120	−323.18297
TS1	−323.18038	−323.17218
TS2	−323.19077	−323.18338
TS3	−323.17456	−323.16698
TS4	−323.19224	−323.18466
TS5	−323.19555	−323.18823
TS6	−323.13533	−323.12779
TS7	−323.15807	−323.15013
TS8	−323.12859	−323.12061
TS9	−246.78984	−246.78282
TS10	−134.59538	−134.58981
TS11	−323.16755	−323.15860
TS12	−323.12756	−323.11879
INT1	−323.20947	−323.19999
INT2	−323.19479	−323.18656
INT3	−323.19791	−323.19005
INT4	−323.17267	−323.16504
INT5	−323.20049	−323.19218
INT6	−323.20258	−323.19282
$NH_2CH_2^+$	−94.88630	−94.88234
CH_2COOH	−228.28873	−228.28346
$NH_3CH_2CH_2^+$	−134.71894	−134.71302
$NH_2CHCH_2CO_2^+$	−321.97184	−321.96430
$NH_2CHCH_2CO^+$	−246.79097	−246.78398
$NH_2CHCH_2^+$	−133.53296	−133.52816
$NH_2CHCH_3^+$	−134.18211	−134.17702
COOH	−189.00211	−188.99795
CO_2	−188.50435	−188.50073
H_2O	−76.38373	−76.37995
H_2	−1.16748	−1.16417

TABLE 2: Theoretical and Experimental IEs of Three Conformers of β-Alanine and AEs of Corresponding Fragments

		IEs/AEs (eV)		
m/z	ion assignments	G3B3	expt.	ref.
89	$G1^+$	8.78	8.86 ± 0.08	8.8 ± 0.1[a]
	$G2^+$	9.15		
	A^+	9.13		
45	$NH_3CH_2CH_2^+$	9.20	9.33 ± 0.08	~8.95[b]
44	$NH_2CHCH_3^+$	10.96	10.20 ± 0.3	
43	$NH_2CHCH_2^+$	9.77	9.32 ± 0.08	9.5 ± 0.2[a]
30	$NH_2CH_2^+$	9.57	9.28 ± 0.08	9.3 ± 0.1[a]

[a] Ref 18. [b] Ref 19.

3.2. Fragmentation Pathways. ***3.2.1. Fragment at m/z = 45 ($NH_3CH_2CH_2^+$).*** In a previous photoionization study performed in the photon energy range of 6−22 eV by Jochims et al.,[18] the authors proposed to assign the fragment at $m/z = 45$ to $COOH^+$. However, based on our G3B3 calculation, the formation of $COOH^+$ from a direct C2−C3 bond cleavage of the G1+ conformer is found to proceed via a transition structure with a barrier of 11.8 eV. Actually the fragment at $m/z = 45$ is attributed to both $COOH^+$ and $NH_3CH_2CH_2^+$. But their appearance energies are different. According to calculation results, $COOH^+$ should be formed at a higher photon energy (>11.8 eV). Hence, we believe that the $m/z = 45$ ion formed from the dissociative photoionization of β-alanine at a photon energy below 11.8 eV should be assigned to $NH_3CH_2CH_2^+$.

If the fragment of $m/z = 45$ is assigned to $NH_3CH_2CH_2^+$, the fragment will be formed by decarboxylation of the G2+ conformer because the conformer has the strongest intermolecular hydrogen bond. As depicted in Scheme 1, the decarboxylation of G2+ involves a C2−C3 bond cleavage and forms the $NH_3CH_2CH_2^+$ cation and carbon dioxide via a transition state (TS4):

SCHEME 1: G3B3 Potential Energy Surface for the Formation of $NH_2CH_2^+$ and $NH_3CH_2CH_2^+$ from the Conformers G1+ and G2+[a]

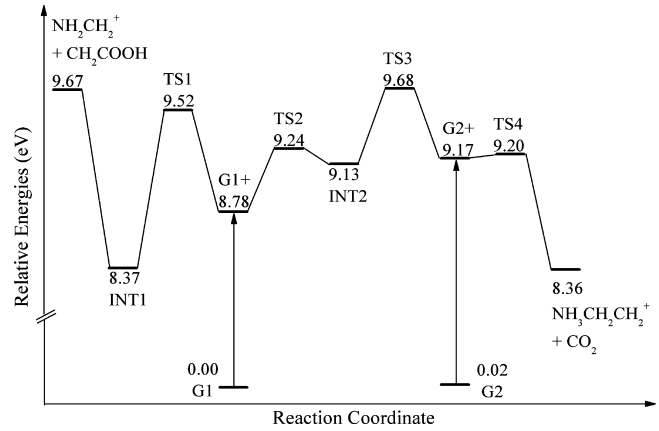

[a] The energy is relative to the ground state G1 conformer of β-alanine.

$$NH_3CH_2CH_2COO^+(G2+) \rightarrow NH_3CH_2CH_2^+ + CO_2,\ AE = 9.20 \qquad (1)$$

At the G3B3 level, the TS4 has an energy barrier of 0.03 eV above the G2+ conformer. The G3B3 IE for the photoionization transition from the G2 conformer of β-alanine to G2+ is 9.15 eV. Thus, the total energy required for the formation of the $NH_3CH_2CH_2^+$ cation and CO_2 fragments from the photodissociative ionization of β-alanine is 9.20 eV (relative to G1). From our experiment, the AE for forming the $m/z = 45$ ion is measured to be 9.33 ± 0.08 eV, which is consistent with the G3B3 predicted value of 9.20 eV after taking into account the uncertainty of our experimental measurement.

However, it is interesting to note that G2+ is not the only conformer that can produce $NH_3CH_2CH_2^+$. Our G3B3 calcula-

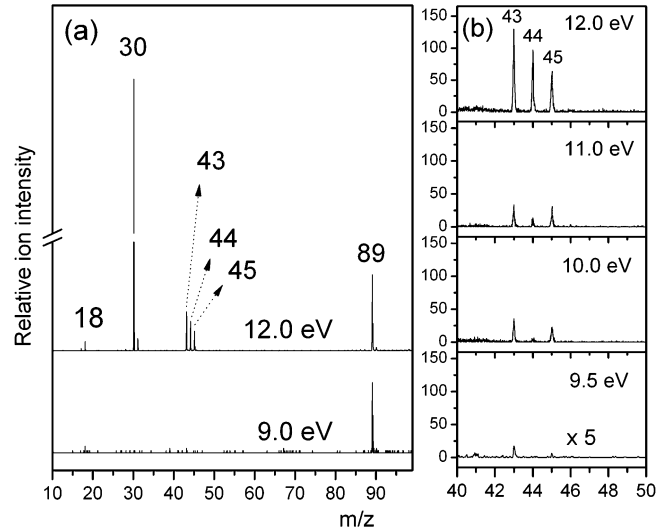

Figure 4. (a) Photoionization mass spectra of β-alanine at photon energies of 9.0 and 12.0 eV. (b) Photoionization mass spectra of β-alanine at photon energies of 9.5, 10.0, 11.0, and 12.0 eV.

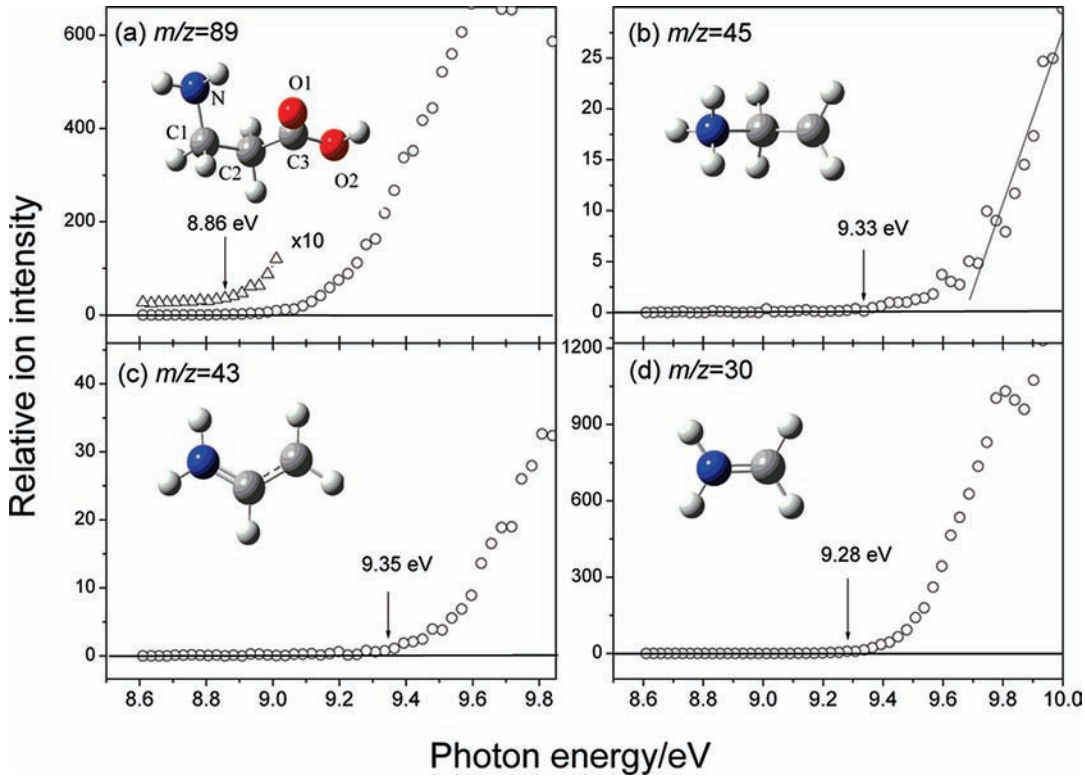

Figure 5. Photoionization efficiency spectra of β-alanine and its fragments.

tions indicate that G1+ may also be a possible precursor for the $NH_3CH_2CH_2^+$ ion and the CO_2 molecule. In Scheme 1, the hydroxyl group of G1+ can undergo an internal rotation about the C2−C3 bond via transition state TS2 to produce intermediate INT2 (0.35 eV above G1+). Then, INT2 proceeds to form G2+ by overcoming a barrier of 0.55 eV (relative to INT2) via TS3. The formation of the $NH_3CH_2CH_2^+$ ion and CO_2 fragments from the G1+ cation requires an overall barrier of 0.9 eV relative to the G1+ (or 9.68 eV relative to G1). As found by Tian, the G1 conformer has the highest abundance among 10 possible low-lying conformers of β-alanine.[15] Thus, the formation of the $NH_3CH_2CH_2^+$ ion ($m/z = 45$) may be mainly originating from the G1+ conformer. Shown in Figure 5b is the PIE spectrum for the $m/z = 45$ ion, in which there is a sharp increase of the ion signal at the photon energy of 9.70 eV and onward. This energy threshold at which the ion signal increases is in coincidence with the overall energy barrier of 9.68 eV for the formation of $m/z = 45$ ion from the G1+ conformer.

3.2.2. Fragment at m/z = 43 ($NH_2CHCH_2^+$). On the basis of the computational results, we suggest that the fragment at $m/z = 43$ may have the chemical formula of $NH_2CHCH_2^+$ because this cation is the most stable isomer on the $C_2NH_5^+$ cationic surface. Our calculations indicate that the $NH_2CHCH_2^+$ ion ($m/z = 43$) and its cofragments may be formed via several pathways beginning with the G1+, G2+, and A+ conformers. For example, starting from the G1+ conformer, two pathways for the formation of $NH_2CHCH_2^+$ ion and cofragments are found, and the corresponding energy profiles are shown in Schemes 2 and 3. In Scheme 2, the G1+ conformer first transfers a hydrogen atom from the C1 to the carboxylic oxygen to form the $NH_2CHCH_2COHOH^+$ cation (a diol cation, INT3) via TS5. The barrier of this hydrogen transfer is 0.33 eV above G1+. Then, $NH_2CHCH_2COHOH^+$ (INT3) proceeds to undergo another hydrogen transfer to yield $NH_2CHCH_2C(H)OOH^+$ (INT4) via TS6 (1.97 eV above G1+). Then INT4 undergoes a C2−C3 bond cleavage to yield the $NH_2CHCH_2^+$ ion and

SCHEME 2: Pathway 1: The G3B3 Potential Energy Surface for the Formation of $NH_2CHCH_2^+$ from the Conformer G1+[a]

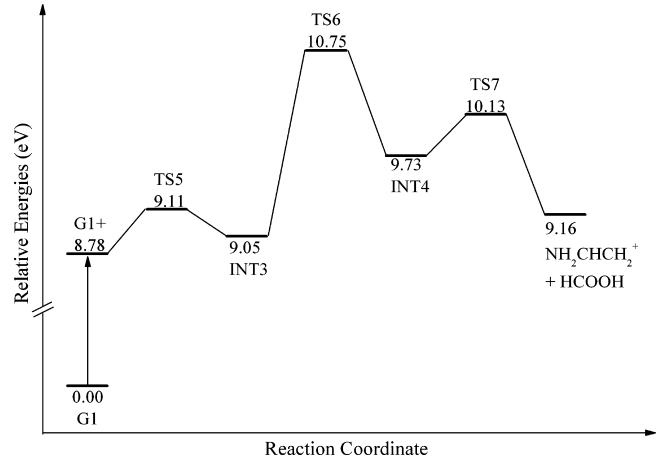

[a] The energy is relative to the ground state G1 conformer of β-alanine.

formic acid (HCOOH). The barrier of the bond cleavage step is 1.35 eV above G1+. The overall barrier for the formation of the $NH_2CHCH_2^+$ ion and HCOOH from the G1+ conformer is 1.97 eV (relative to G1+) or 10.75 eV (relative to G1). Shown in Scheme 3 is the alternative pathway for the formation of the $NH_2CHCH_2^+$ ion: INT3 may convert into INT5 (through an internal rotation of the -OH group), and the INT5 then undergoes a hydrogen transfer between the two -OH groups via TS8. The barrier of this hydrogen transfer is 2.15 eV above that of the G1+ conformer. This hydrogen transfer process, accompanied by the departure of a water molecule from the TS8, yields the $NH_2CHCH_2CO^+$ ion. This ion may then undergo a direct bond cleavage to form the $NH_2CHCH_2^+$ ion and CO_2 via TS9 with a miniscule barrier of 0.03 eV (relative to $NH_2CHCH_2CO^+$ +

SCHEME 3: Pathway 2: The G3B3 Potential Energy Surface for the Formation of $NH_2CHCH_2^+$ from the Conformer G1+[a]

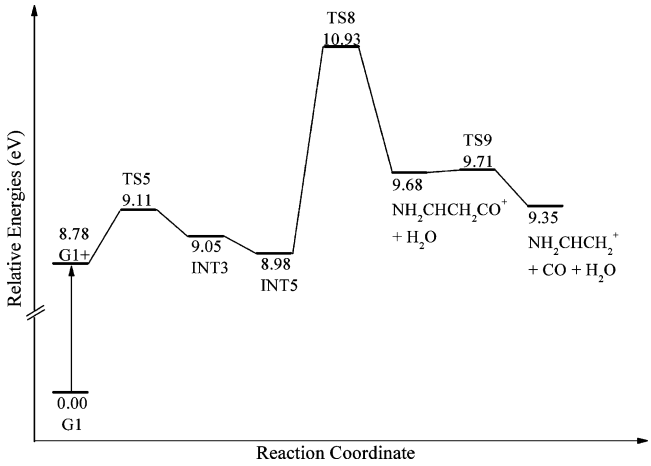

[a] The energy is relative to the ground state G1 conformer of β-alanine.

SCHEME 4: G3B3 Potential Energy Surface for the Formation of $NH_2CHCH_2^+$ from the Conformer G2+[a]

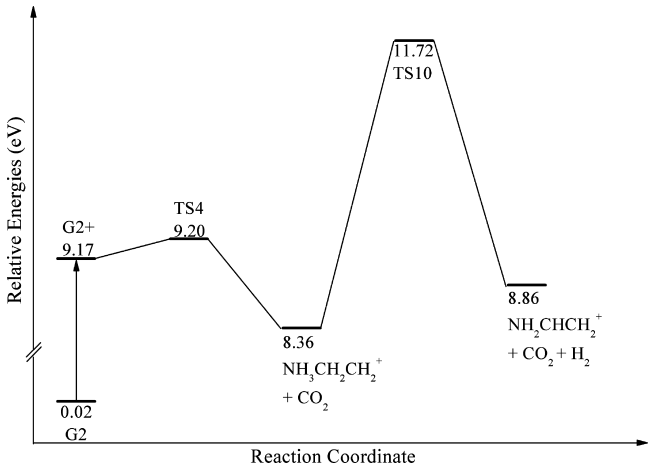

[a] The energy is relative to the ground state G1 conformer of β-alanine.

H_2O). The overall barrier for the formation of the $NH_2CHCH_2^+$ ion and CO + H_2O from the G1+ conformer is 2.15 eV (relative to G1+) or 10.93 eV (relative to G1), which is higher than the overall barrier for the formation of the $NH_2CHCH_2^+$ ion and HCOOH by 0.18 eV.

As mentioned previously, the $NH_2CHCH_2^+$ cation may also originate from the G2+ ($NH_3CH_2CH_2COO^+$) conformer through two successive elimination processes. As shown in Scheme 4, the G2+ conformer can first decarboxylate to yield $NH_3CH_2CH_2^+$ and CO_2 via TS4; the dissociated $NH_3CH_2CH_2^+$ ion then yields $NH_2CHCH_2^+$ and H_2 by a hydrogen elimination via TS10. The overall barrier for the formation of the $NH_2CHCH_2^+$ ion and CO_2 + H_2 from the G2+ conformer is 2.55 eV (relative to G2+) or 11.72 eV (relative to G1).

No intramolecular hydrogen bond is found in conformer A+. The formation pathway for the $NH_2CHCH_2^+$ ion and CO + H_2O from the A+ conformer is displayed in Scheme 5. The A+ conformer first undergoes an intramolecular hydrogen transfer from C1 to the hydroxyl oxygen via TS11 to yield the $NH_2CHCH_2CO^+\cdots H_2O$ intermediate complex (INT6). Then INT6 becomes fully dissociated, and the dissociated

SCHEME 5: G3B3 Potential Energy Surface for the Formation of $NH_2CHCH_2^+$ and $NH_2CH_2^+$ from the Conformer A+[a]

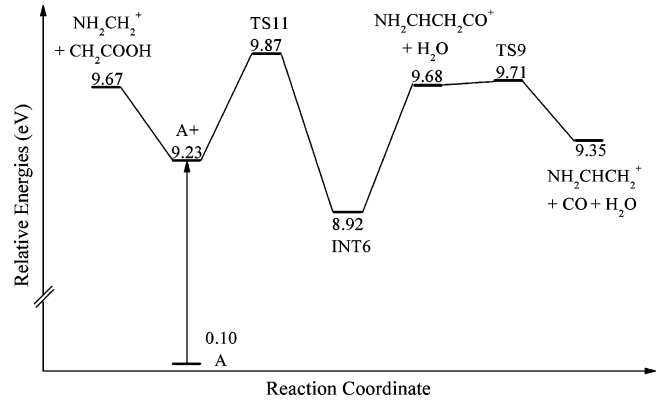

[a] The energy is relative to the ground state G1 conformer of β-alanine.

$NH_2CHCH_2CO^+$ ion undergoes CO elimination via TS9 to form $NH_2CHCH_2^+$ and CO. The overall barrier for the dissociation pathway from the A+ conformer yielding the $NH_2CHCH_2^+$ ion and CO + H_2O is 0.64 eV (relative to A+) or 9.87 eV (relative to G1). All four formation pathways of $NH_2CHCH_2^+$ ion and cofragments from the conformers G1+, G2+, and A+ and the corresponding AEs for $NH_2CHCH_2^+$ are listed in eqs 2−5:

$$NH_2CH_2CH_2COOH^+(G1+) \rightarrow NH_2CHCH_2^+ + HCOOH,\ AE = 10.75 \quad (2)$$

$$NH_2CH_2CH_2COOH^+(G1+) \rightarrow NH_2CHCH_2^+ + CO + H_2O,\ AE = 10.93 \quad (3)$$

$$NH_3CH_2CH_2COO^+(G2+) \rightarrow NH_2CHCH_2^+ + H_2 + CO_2,\ AE = 11.72 \quad (4)$$

$$NH_2CH_2CH_2COOH^+(A+) \rightarrow NH_2CHCH_2^+ + CO + H_2O\ AE = 9.87 \quad (5)$$

The PIE spectrum of $NH_2CHCH_2^+$, presented in Figure 5c, exhibits an onset of ion signals at the photon energy of 9.32 ± 0.08 eV. The G3B3 AE values for the $NH_2CHCH_2^+$ ion from different fragmentation pathways range from 9.87 to 11.72 eV, which are obviously much higher than the experimental result. The large discrepancy between the calculated values and experimental measurement may be due to temperature effects and numerous possible conformations of the β-alanine. The numerous possible conformations of the β-alanine would make it more difficult to find a reaction pathway with lower activation energy. However, there is another AE value (9.5 ± 0.2 eV) obtained from the photoionization mass spectrometric experiment by Jochims et al.[16] Although the uncertainty of the previous AE measurements for $m/z = 45$ is larger than our current one (±0.08 eV), this AE value still agrees well with our experimental AE and the (lowest) G3B3 AE values, after taking the error bars into account.

3.2.3. Fragment at m/z = 30 ($NH_2CH_2^+$). The fragment at $m/z = 30$ corresponds to $NH_2CH_2^+$, which is produced via the direct loss of a CH_2COOH radical from $NH_2CH_2CH_2COOH^+$ (G1+). The formaldehyde cation (H_2CO^+) has the same m/z = 30 as the $NH_2CH_2^+$. However, the formation of formaldehyde should involve H migration in the parent cation followed by the C−O and C−C bond cleavages. Thus, we expect that the

SCHEME 6: G3B3 Potential Energy Surface for the Formation of $NH_2CHCH_3^+$ from the Conformer G1+[a]

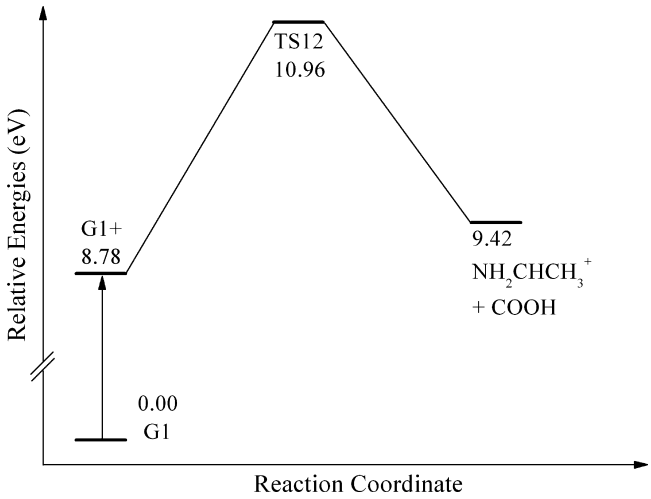

[a] The energy is relative to the ground state G1 conformer of β-alanine.

energy required for the formation of the H_2CO^+ cation is relatively high. At a lower photon energy, the formation for a fragment ion at $m/z = 30$ as $NH_2CH_2^+$ should be energetically more favorable. As shown in the photoionization mass spectra of β-alanine, the $NH_2CH_2^+$ ion has the strongest ion intensity, which is mainly due to the delocalization of lone-pair electrons along the C−N bond, making this fragment extremely stable. This observation is similar to the previous results using photoionization[14] and EI methods.[30] Most of the conformers except G2+ contribute directly to the formation of the $NH_2CH_2^+$ ion. For example, as shown in Scheme 1, the G1+ conformer may undergo a direct C1−C2 bond cleavage to yield an ion complex intermediate $NH_2CH_2^+\cdots HOOCCH_2$ (INT1) via TS1. Then INT1 may dissociate into $NH_2CH_2^+$ and CH_2COOH. The AE energy (eq 6) for the formation of $NH_2CH_2^+ + CH_2COOH$ from the G1+ conformer is 0.89 eV (relative to G1+) or 9.67 eV (relative to G1). The calculated AE value (9.67 eV) is higher than our experimental value of 9.28 ± 0.08 eV. The AE for the formation of $NH_2CH_2^+ + CH_2COOH$ from the A+ conformer (eq 7 and Scheme 5) is 9.57 eV (relative to that of A), which is about 0.29 eV higher than the experimental measurement. Nevertheless, the measurement is consistent with the results reported previously.[18,20] The PIE spectrum of the $NH_2CH_2^+$ ion shows a relative gradual increase from onset (9.28 eV) and afterward rises sharply at around 9.56 eV. This behavior is also observed in similar studies on other amino acids.[12] Jochims et al. attributed this long tail with low intensity to the ion pair formation process $NH_2CH_2CH_2COOH \rightarrow NH_2CH_2^+ + CH_2COOH^-$.[18]

$$NH_2CH_2CH_2COOH^+(G1+) \rightarrow NH_2CH_2^+ + CH_2COOH \quad AE = 9.67 \qquad (6)$$

$$NH_2CH_2CH_2COOH^+(A+) \rightarrow NH_2CH_2^+ + CH_2COOH \quad AE = 9.57 \qquad (7)$$

3.2.4. Fragments at m/z = 44 ($NH_2CHCH_3^+$). At first sight, fragment at $m/z = 44$ is assigned to $NH_2CH_2CH_2^+$ as it can be readily produced from a simple C2−C3 bond cleavage.[18] However, our G3B3 results predict that the $NH_2CHCH_3^+$ ion is more stable than the $NH_2CH_2CH_2^+$ isomer by 2.6 eV. As a result, we believe that the $m/z = 44$ fragment should be assigned to the $NH_2CHCH_3^+$ ion (eq 8). The formation process for the $NH_2CHCH_3^+$ ion and cofragment is predicted to be the following. First, the G1+ conformer undergoes a 1,2-hydrogen transfer forming $NH_2CHCH_3COOH^+$ (via TS12); this hydrogen transfer is immediately followed by the rupture of the C2−C3 bond yielding the $NH_2CHCH_3^+$ ion and COOH radical (the $NH_2CHCH_3COOH^+$ is an unstable species). The reaction profile is depicted in Scheme 6, and the G3B3 AE value is calculated to be 10.96 eV. The experimental AE value of $NH_2CHCH_3^+$ is estimated to be 10.2 ± 0.3 eV with a relatively large error bar.

$$NH_2CH_2CH_2COOH^+(G1+) \rightarrow NH_2CHCH_3^+ + COOH \quad AE = 10.96 \qquad (8)$$

4. Conclusions

The photoionization mass spectra and PIE spectra of β-alanine are obtained using IR laser desorption combined with tunable synchrotron VUV photoionization mass spectrometry. Fragments at $m/z = 45$, 44, 43, and 30 are attributed to the $NH_3CH_2CH_2^+$, $NH_2CHCH_3^+$, $NH_2CHCH_2^+$, and $NH_2CH_2^+$ cations, respectively. The IE of β-alanine and AEs of fragment ions are obtained from the PIE measurements, and the photodissociation pathways for the formation of fragments ions are then compared with the G3B3 theoretical predictions.

Conformation-specific dissociation channels of β-alanine cation are established. In addition to the direct decarboxylation process of G2+, the conformer G1+ is found to be a more dominant precursor in forming $NH_3CH_2CH_2^+$ with the photon energy below 11.8 eV. Cation $NH_2CHCH_2^+$ may be produced from the dissociations of the conformers G1+, G2+, and A+ via different pathways. As the most abundant fragment, $NH_2CH_2^+$ is resulted via a direct loss of the neutral CH_2COOH fragment from $NH_2CH_2CH_2COOH^+$, which may be produced by the ion pair formation of the parent molecule prior to ionization. Cation $NH_2CHCH_3^+$ ($m/z = 44$) is produced from C2−C3 bond cleavage after the hydrogen transfer process from C1 to C2, instead of from a simple C2−C3 bond cleavage.

Acknowledgment. We thank Professor Wai-Kee Li and Dr. Yuyang Li for useful discussions. This work is supported by grants from the Chinese Academy of Sciences (YZ200764), the Natural Science Foundation of China (10705026 and 10805047), the Ministry of Science and Technology of China (2007CB815204), and the China Postdoctoral Science Foundation (20070410793 and 20070420726). The calculation work described in this article is supported by a grant from the Research Grants Council of the Hong Kong Special Administrative Region, China (CityU 101507, to K.-C.L.).

References and Notes

(1) Eliel, E. L.; Lukach, C. A. *J. Am. Chem. Soc.* **1957**, *79*, 5986.
(2) Goez, M. *Angew. Chem., Int. Ed.* **2003**, *42*, 2336.
(3) Park, S. T.; Kim, S. K.; Kim, M. S. *J. Chem. Phys.* **2001**, *114*, 5568.
(4) Park, S. T.; Kim, S. K.; Kim, M. S. *Nature (London)* **2002**, *415*, 306.
(5) Khriachtchev, L.; Macoas, E.; Pettersson, M.; Rasanen, M. *J. Am. Chem. Soc.* **2002**, *124*, 10994.
(6) Kim, M. H.; Shen, L.; Tao, H. L.; Martinez, T. J.; Suits, A. G. *Science* **2007**, *315*, 1561.
(7) Dian, B. C.; Clarkson, J. R.; Zwier, T. S. *Science* **2004**, *303*, 1169.
(8) Nelson, G.; Chandrashekar, J.; Hoon, M.; Feng, L. X.; Zhao, G.; Ryba, N. J. P.; Zuker, C. S. *Nature (London)* **2002**, *416*, 199.
(9) Brack, A., Ed. *The Molecular Origins of Life*; Cambridge University Press: Cambridge, UK, 1998.
(10) Shemesh, D.; Gerber, R. B. *J. Chem. Phys.* **2005**, *122*, 241104.
(11) Vorsa, V.; Kono, T.; Willey, K. F.; Winograd, N. *J. Phys. Chem. B* **1999**, *103*, 7889.

(12) Lago, A. F.; Coutinho, L. H.; Marinho, R. R. T.; de Brito, A. N.; de Souza, G. G. B. *Chem. Phys.* **2004**, *307*, 9.
(13) Wilson, K. R.; Jimenez-Cruz, M.; Nicolas, C.; Belau, L.; Leone, S. R.; Ahmed, M. *J. Phys. Chem. A* **2006**, *110*, 2106.
(14) Ehrenfreund, P.; Glavin, D. P.; Botta, O.; Cooper, G.; Bada, J. L. *Proc. Natl. Acad. Sci. U.S.A* **2001**, *98*, 2138.
(15) Tian, S. X. *J. Phys. Chem. A* **2006**, *110*, 3961.
(16) Sanz, M. E.; Lesarri, A.; Pena, M. I.; Vaquero, V.; Cortijo V.; Lopez, J. C.; Alonso, J. L. *J. Am. Chem. Soc.* **2006**, *128*–3812.
(17) McGlone, S. J.; Godfrey, P. D. *J. Am. Chem. Soc.* **1995**, *117*, 1043.
(18) Jochims, H.; Schwell, M.; Chotin, J.; Clemino, M.; Dulieu, F.; Baumgärtel, H.; Leach, S. *Chem. Phys.* **2004**, *298*, 279.
(19) Choi, K. W.; Ahn, D. S.; Lee, J. H.; Kim, S. K. *Chem. Commun.* **2007**, 1041.
(20) Schwell, M.; Jochims, H. W.; Baumgarel, H.; Dulieu, F.; Leach, S. *Planet. Space Sci.* **2006**, *54*, 1073.
(21) Bari, S.; Sobocinski, P.; Postma, J.; Alvarado, F.; Hoekstra, R.; Bernigaud, V.; Manil, B.; Rangama, J.; Huber, B.; Schlathölter, T. *J. Chem. Phys.* **2008**, *128*, 074606.
(22) Pan, Y.; Zhang, L. D.; Zhang, T. C.; Guo, H. J.; Hong, X.; Sheng, L. S.; Qi, F. *Phys. Chem. Chem. Phys.* **2009**, *11*, 1189.
(23) Pan, Y.; Zhang, T. C.; Hong, X.; Zhang, Y. W.; Sheng, L. S.; Qi, F. *Rapid Commun. Mass Spectrom.* **2008**, *22*, 1691.
(24) Pan, Y.; Zhang, T. C.; Guo, H. J.; Hong, X.; Qi, F. *J. Mass Spectrom.* **2008**, *43*, 1701.
(25) Pan, Y.; Yin, H.; Zhang, T. C.; Guo, H. J.; Sheng, L. S.; Qi, F. *Rapid Commun. Mass Spectrom.* **2008**, *22*, 2515.
(26) Baboul, A. G.; Curtiss, L. A.; Redfern, P. C.; Raghavachari, K. *J. Chem. Phys.* **1999**, *110*, 7650.
(27) Frisch, M. J. et al. *Gaussian 03*, revision C. 02;Gaussian Inc.: Wallingford, CT, 2004.
(28) Yang, B.; Huang, C. Q.; Wei, L. X.; Wang, J.; Sheng, L. S.; Zhang, Y. W.; Qi, F.; Zheng, W. X.; Li, W. K. *Chem. Phys. Lett.* **2006**, *423*, 321.
(29) Wei, L. X.; Yang, B.; Yang, R.; Huang, C. Q.; Wang, J.; Shan, X. B.; Sheng, L. S.; Zhang, Y. W.; Qi, F.; Lam, C. S.; Li, W. K. *J. Phys. Chem. A* **2005**, *109*, 4231.
(30) Linstrom, P. J.; Mallard, W. J. *NIST Chemistry Webbook*, Number 69; National Institute of Standard and Technology: Gaithersburg, MD, 2005. http://webbook.nist.gov.
(31) Jackschath, C.; Rabin, I.; Schulze, W. *Z. Phys. D* **1992**, *22*, 517.
(32) Guyon, P. M.; Berkowitz, J. *J. Chem. Phys.* **1971**, *54*, 1814.
(33) Chupka, W. A. *J. Chem. Phys.* **1971**, *54*, 1936.

JP9002565